

## New features in the radio-emission of very inclined air-showers

Simon Chiche,<sup>a,\*</sup> Chao Zhang,<sup>c,b,i</sup> Kumiko Kotera,<sup>a,j</sup> Tim Huege,<sup>c,j</sup> Krijn D. de Vries,<sup>f</sup> Felix Schlüter<sup>c,h</sup> and Matias Tueros<sup>d,e,a</sup>

<sup>a</sup>Sorbonne Université, CNRS, UMR 7095, Institut d'Astrophysique de Paris, 98 bis bd Arago, 75014 Paris, France

<sup>b</sup>Kavli institute for astronomy and astrophysics, Peking University, Beijing, China

<sup>c</sup>Institute for Astroparticle Physics (IAP), Karlsruhe Institute of Technology, Karlsruhe, Germany

<sup>d</sup>IFLP - CCT La Plata - CONICET, Casilla de Correo 727 (1900) La Plata, Argentina

<sup>e</sup>Depto. de Física, Fac. de Cs. Ex., Universidad Nacional de La Plata, Casilla de Correo 67 (1900) La Plata, Argentina

<sup>f</sup>Vrije Universiteit Brussel (VUB), Dienst ELEM, Pleinlaan 2, B-1050, Brussels, Belgium

<sup>j</sup>Astrophysical Institute, Vrije Universiteit Brussels, Pleinlaan 2, 1050 Brussels, Belgium

<sup>g</sup>Sorbonne Université, Université Paris Diderot, Sorbonne Paris Cité, CNRS, Laboratoire de Physique Nucléaire et de Hautes Energies (LPNHE), Paris, France

<sup>h</sup>Universidad Nacional de San Martín, Instituto de Tecnologías en Detección y Astropartículas, Buenos Aires, Argentina

<sup>i</sup>Department of Astronomy, School of Physics, Peking University, Beijing, China

E-mail: [simon.chiche@iap.fr](mailto:simon.chiche@iap.fr)

To probe the sources of ultra-high energy cosmic-rays, next-generation ultra-high-energy detectors such as GRAND, BEACON, and the radio upgrade of AugerPrime, will target the detection of cosmic-ray, gamma-ray and neutrino showers with inclined arrival detections. These inclined showers develop higher in the atmosphere and over longer distances than vertical ones, which affects the radio emission in non-trivial ways. Using Monte-Carlo simulations, we evidence two major novel features of cosmic-ray inclined showers: a significant drop of more than one order of magnitude in the radiation energy and a new polarization pattern. We explain the former by a coherence loss in the radio emission of inclined air-showers, while the latter possibly indicates a synchrotron emission becoming relevant at large zenith angles. If confirmed, these two effects could have a significant impact on the detection and reconstruction strategies of next-generation radio experiments.

38th International Cosmic Ray Conference (ICRC2023)  
26 July - 3 August, 2023  
Nagoya, Japan



\*Speaker

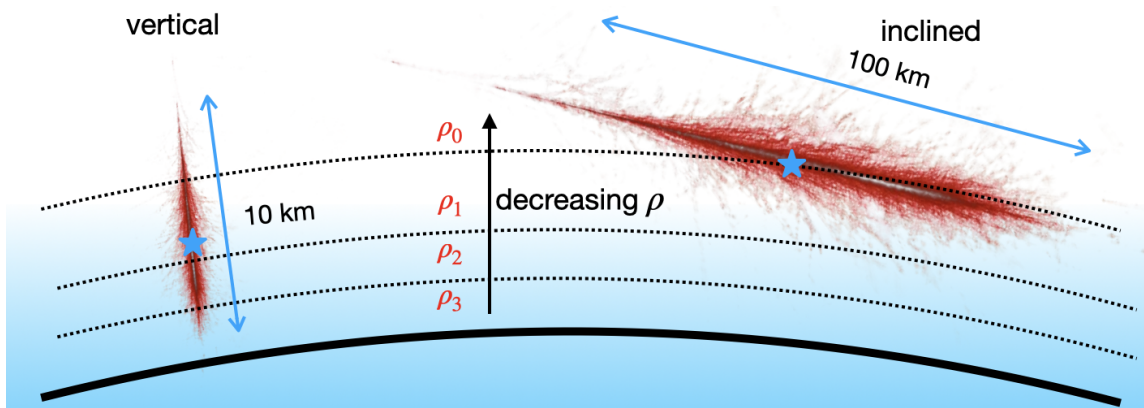


**Figure 1:** (Not to scale) Sketch of a vertical and an inclined air-shower. The blue star indicates the  $X_{\max}$  position of each shower. Inclined air-showers develop at higher altitude, hence lower density in the atmosphere and over longer distances than vertical ones. The sketch also shows that Earth curvature and the asymmetry of the atmospheric density around the shower axis should be considered for inclined air-showers.

## 1. Introduction

Radio detection of high-energy astroparticles has been extensively studied over the past decade. Experimental progresses in cosmic-ray detection from CODALEMA [1], LOPES [2], AERA [3] and LOFAR [4] fed the development of accurate Monte-Carlo simulations and of theoretical models, providing a deep understanding of the radio emission processes [5, 6]. The radio emission from vertical showers is now well understood and can be interpreted as the coherent sum of two main mechanisms: the geomagnetic emission, coming from the deflection of charged particles in the shower by the Earth’s magnetic field and the time variation of the resulting transverse current; and the charge-excess emission coming from the accumulation of negative charges in the shower front due to the ionization of air-atoms. The objective of the community is now to increase the sensitivity and to target other messengers, gamma-rays and neutrinos, at ultra-high-energy (UHE). This motivates the development of next generation experiments, with gigantic detection surfaces and more efficient detection methods, with a focus on radio techniques to address the low fluxes at UHE [7, 8]. Inclined air-showers are particularly well-suited for this purpose as their large radio footprints allow us to sample the signal with sparse arrays, i.e., to cover large surfaces at low costs. Yet, their radio emission exhibits numerous features that differentiate them from vertical showers making their understanding challenging with the existing theoretical models [9, 10, 22]. In Section 2 we present the main characteristics of inclined showers. We then evidence in Section 3 two new features of inclined air-shower radio emission: a suppression of the radiated energy and a new polarization signature at low densities and high magnetic field amplitude. Eventually in Section 4, we discuss how the current theoretical models should be refined to account for these two effects that we link respectively to a loss of coherence and a synchrotron component. The text from Sections 2 and 3 directly follows what was presented in [21].

## 2. The challenge of inclined air-showers

When a particle cascade develops in the atmosphere, the total number of particles increases until it reaches a maximum, and then decreases. The atmospheric grammage  $X_{\max}$  at which the

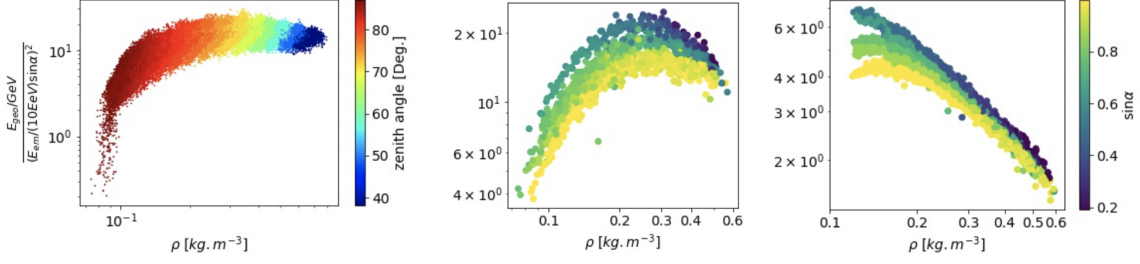


**Figure 2:** (Left) Full band radiated geomagnetic energy as a function of air-density from ZHAireS simulations with GRAND magnetic field configuration ( $B = 55 \mu\text{T}$ ,  $i = 60.79^\circ$ ). The colors code for the zenith angle. (Middle) Radiated energy, filtered in the 50 – 200 MHz band, as a function of air-density from CoREAS simulations with GRAND magnetic field. The colors code for  $\sin \alpha$ , with  $\alpha$  the geomagnetic angle. The plot shows a similar trend to the results with ZHAireS simulations, i.e., an increase of the radiated energy followed by a drop at the lowest densities. The colors attest of a deviation from a scaling of the radiated energy as  $\sin^2 \alpha$ . (Right) Radiated energy as a function of air-density from CoREAS simulations with AERA magnetic field configuration ( $B = 24.6 \mu\text{T}$ ,  $i = -35.2^\circ$ ) and frequency band (30 – 80 MHz). The plot shows almost no cut-off at low densities and the radiated energy roughly scales in  $\sin^2 \alpha$  (except at the lowest densities).

maximal number of particles is reached depends mainly on the particle nature and not on its arrival direction. As a consequence, inclined cosmic-ray air-showers will develop in higher, hence lower density atmosphere than vertical ones. This is illustrated in Fig. 1, where we highlight some differences between vertical and inclined showers that are relevant in our framework. It can be seen that inclined showers develop over much longer distances than vertical ones, resulting in a more diluted signal. This long development also implies that Earth curvature has to be taken into account when modeling the atmosphere and setting the antenna positions on ground. The inclined shower trajectory will also create an asymmetry of the radio footprint related to a different integrated refractive index and arrival time of the signal between "early" antennas (located below the shower axis) and "late" antennas (above the shower axis) [11, 12]. Eventually, the lower density for inclined showers should impact the radio emission processes as discussed in [9, 10, 15]. In the next Section we aim at characterizing quantitatively the impact of air-density on the radio emission with Monte-Carlo simulations.

### 3. Radio signal dependency with air-density

#### 3.1 Evidence for a suppression of the radiated energy of inclined air-showers

To compute the radio-signal dependency with air-density, we calculated with ZHAireS Monte-Carlo simulations [13] the radiated energy for showers with various inclination. We used a set of  $\sim 10\,000$  showers with antennas on a star-shape layout, with zenith angle  $\theta$  between  $[40^\circ - 80^\circ]$ , various azimuth angles  $\phi$  between  $[0^\circ - 360^\circ]$  and primary particle energy  $\mathcal{E}$  between  $[0.1 - 4]$  EeV. The magnetic field amplitude is set to  $B_{\text{geo}} = 55 \mu\text{T}$  and its inclination to  $i = 60.79^\circ$  following the values at the GRAND experiment candidate site, in Dunhuang, China.

As discussed in [9], for inclined showers, the charge-excess contribution to the radio signal becomes negligible relatively to the geomagnetic one. We can therefore assume that the radiated geomagnetic energy,  $E_{\text{rad geo}}$  is an accurate proxy for the total radiated energy by the air-shower.

$E_{\text{rad,geo}}$  is calculated following the method proposed in [14], i.e., by integrating, in space, the  $\mathbf{v} \times \mathbf{B}$  component of the radio energy fluence  $f_{\mathbf{v} \times \mathbf{B}} = \epsilon_0 c \Delta t \sum_i |E_{\mathbf{v} \times \mathbf{B}}(t_i)|^2$  (where  $E_{\mathbf{v} \times \mathbf{B}}$  is the the  $\mathbf{v} \times \mathbf{B}$  component of the electric field, where the sum is performed over the whole time window of length  $\Delta t$ ,  $\epsilon_0$ , the vacuum permittivity and  $c$  the speed of light in vacuum) using antennas located on the  $\mathbf{v} \times (\mathbf{v} \times \mathbf{B})$  axis and assuming a radial symmetry of the radio signal. Finally, we divide the result by  $\mathcal{E}^2 \sin^2 \alpha$ , (with  $\alpha$ , the geomagnetic angle and  $\mathcal{E}$  the shower electromagnetic energy) to correct the result from any dependency with the primary energy and azimuth angle. We get:

$$E_{\text{geo}}^{\text{rad}}(\epsilon, \Phi, \theta) = \frac{2\pi\epsilon_0 c \Delta t}{\mathcal{E}^2 \sin^2 \alpha} \int_0^{+\infty} \sum_i |E_{\mathbf{v} \times \mathbf{B}}(r, t_i)|^2 r \, dr \quad (1)$$

Here,  $r \, dr$  (with  $r$ , the distance of a given antenna from the shower core) can be re-expressed as  $D_{X_{\text{max}}}^2 \omega \, d\omega$  with  $D_{X_{\text{max}}}$ , the distance between  $X_{\text{max}}$  and the shower core, and  $\omega$ , the angular deviation to the shower axis from  $X_{\text{max}}$ , such as  $\tan(\omega) \sim \omega = r/D_{X_{\text{max}}}$ . It should be noted that rigorously, the  $X_{\text{max}}$ -observer distance should be used instead of the  $X_{\text{max}}$ -shower core distance. However, in practice the radio footprint extends only to small viewing angles ( $\sim$  up to  $3^\circ$ ) and we can thus assume that both quantities are roughly equal.

The result is displayed as a function of air-density or zenith angle, on the left-hand of Fig. 2, for the full band electric field. It can be seen that when going from high to low densities, the radiated energy first slightly increases (for  $\theta$  between  $40^\circ$  to  $70^\circ$ ) and then decreases (for  $\theta$  above  $70^\circ$ ), with a cut-off of more than 1.5 orders of magnitude for the most inclined showers. This result is confirmed with CoREAS simulations [16] on the middle panel of Fig. 2, where a similar behavior is observed in the GRAND frequency band (50 – 200 MHz). On the other hand, in the right panel of Fig. 2, we present the radiated energy as a function of air-density using this time the magnetic field configuration and frequency band of the Auger site AERA in Malargüe ( $B = 24.6 \mu\text{T}$ ,  $i = -35.2^\circ$ ). It should be noted that although different frequency bands are depicted on the 3 plots, only a mild deviation from the filtering is expected between the full band, GRAND and Auger case, as the peak of the radio signal spectrum (around tens of MHz) is included in each of the considered bands. In the right panel of Fig. 2, it can be seen that when lowering the density, the radiated energy almost always increases and only a mild cut-off is observed for  $\rho < 0.1 \text{ kg m}^{-3}$ . This decrease and the associated cut-off of the radiated energy for GRAND magnetic field values are unexpected features that are not predicted by any existing macroscopic description of the radio emission. Indeed, in the classical picture, one would expect that when lowering the density it would increase the mean free path of collision of positrons and electrons in the shower, resulting in a stronger current and a stronger geomagnetic emission. However, our results suggest that for low air-densities coupled with high magnetic field values, the current paradigm of the radio emission are no longer valid and should be refined to account for these new effects.

### 3.2 Evidence for a new polarization signature

We also studied, with Monte-Carlo simulations, how the polarization should be modified for inclined air-showers. On the left panel of Fig. 3 we represented, from ZHAireS simulations, the  $\mathbf{v} \times (\mathbf{v} \times \mathbf{B})$  component of the full band electric field ( $E_{\mathbf{v} \times \mathbf{v} \times \mathbf{B}}$ ), for a shower with zenith angle  $\theta = 38^\circ$ . As the transverse current emission is polarized along the  $-\mathbf{v} \times \mathbf{B}$  direction, the only contribution to  $E_{\mathbf{v} \times \mathbf{v} \times \mathbf{B}}$  should come from the charge-excess emission. This is confirmed by the

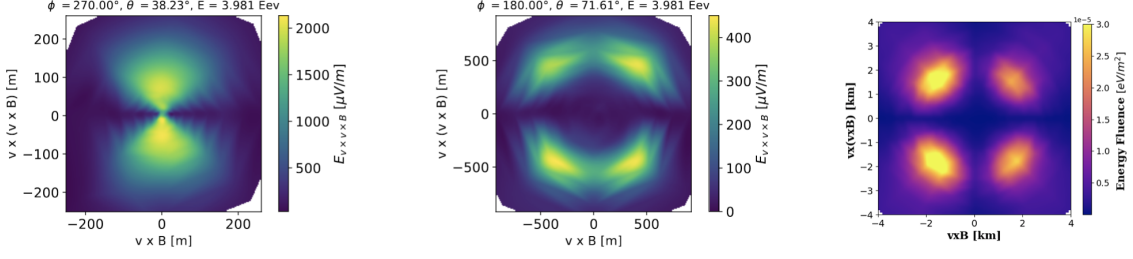


**Figure 3:** Projected component of the full band peak electric field along  $\mathbf{v} \times (\mathbf{v} \times \mathbf{B})$  for (left), a ZHAireS simulation with zenith angle  $\theta = 38^\circ$ , (middle), a ZHAireS simulation with zenith angle  $\theta = 72^\circ$ . (Right)  $\mathbf{v} \times (\mathbf{v} \times \mathbf{B})$  component of the energy fluence filtered in the [50-200] MHz band from a CoREAS simulation with zenith angle  $\theta = 65^\circ$ . The results are shown in the  $[\mathbf{v} \times \mathbf{B}; \mathbf{v} \times (\mathbf{v} \times \mathbf{B})]$  plane, perpendicular to the shower axis, where  $\mathbf{v}$  and  $\mathbf{B}$  are unitary vectors. The left-hand plot shows a pattern that follows the usual projection of the charge excess emission along the  $\mathbf{v} \times (\mathbf{v} \times \mathbf{B})$  axis. The middle and the right-hand plot however, show a polarization pattern that is not predicted by the current paradigm of geomagnetic plus charge excess emission and hints toward a new emission taking over the charge excess for inclined air-showers.

footprint that follows the expected pattern for the  $\mathbf{v} \times (\mathbf{v} \times \mathbf{B})$  projection of the charge excess, i.e., an emission that is peaked along the  $\mathbf{v} \times (\mathbf{v} \times \mathbf{B})$  axis and reaches 0 along the  $\mathbf{v} \times \mathbf{B}$  axis. In Fig. 3, we represent the  $\mathbf{v} \times (\mathbf{v} \times \mathbf{B})$  component of the electric field (middle plot) and the energy fluence (right-hand plot) respectively for ZHAireS and CoREAS simulations of a shower with zenith angle  $\theta = 72^\circ$  (respectively  $\theta = 85^\circ$ ). We see with both simulations, that the emission follows a "clover-leaf pattern", i.e., it is peaked on the diagonal axes and vanishes along the  $\mathbf{v} \times \mathbf{B}$  and  $\mathbf{v} \times (\mathbf{v} \times \mathbf{B})$  directions. This pattern, that is observed for inclined air-shower simulations, can not be described by the current paradigm of the radio emission assuming only a transverse current and charge excess contribution. It can only be explained by a weaker charge excess emission (as discussed in [9]) and the emergence of new type of emission dominant over the charge excess for low air-densities. This new polarization pattern could potentially come from synchrotron emissions as suggested by geo-synchrotron models which predicted a clover-leaf like pattern, similar to the one observed in Fig. 3, in the GHz band for vertical showers [19]. In the next Section, we propose a model to characterize this new emission.

#### 4. Refined modeling of the radio emission

In the previous section, we evidenced, with Monte-Carlo simulations, two new effects in the radio emission of air-showers for low air-density,  $\rho_{\text{air}}$ , and high Earth magnetic field amplitude,  $B_{\text{geo}}$ : a suppression of the radiated energy and a new polarization pattern. These effects become significant for inclined ( $\theta \gtrsim 70^\circ$ ) air-showers, but are not predicted by the analytical macroscopic descriptions of the radio emission. In this section, we propose a refined modeling of the radio emission to account for these new effects.

##### 4.1 Conditions for a coherent signal in the radio emission of air-showers

As discussed in Section 3.1, the suppression in the radiation energy of inclined air-showers appears to be linked to a low air-density, combined with a high magnetic field amplitude. This suggests that it could be related to the shower lateral extent,  $L_{\text{lat}}$ , which itself depends on both of these parameters. Indeed, lowering the air-density should increase the mean free path of collision

of electrons and positrons, while increasing the magnetic field should enhance the deflections, both resulting in a larger shower lateral extent. If we assume that the radio emission is emitted around  $X_{\max}$ , then we can construct with  $L_{\text{lat}}$  the spatial coherence length given by  $L_c = \lambda D_{X_{\max}}/L_{\text{lat}}$ , where  $\lambda$  is the wavelength of the emission and  $D_{X_{\max}}$ , the distance between  $X_{\max}$  and the shower core. This condition arises from the fact that if particles in a plane perpendicular to the shower axis at  $X_{\max}$  radiate in phase, then the only phase difference at the observer position will come from the different particle locations, i.e., from the plane lateral extension. The spatial coherence length hence allows us to quantify if an observer located at  $D_{X_{\max}}$  from the plane, will receive radiation in phase or not, depending on whether we have  $L_{\text{lat}} < L_c$  or  $L_{\text{lat}} > L_c$ .

To evaluate the coherence length,  $D_{X_{\max}}$  can be computed from Monte-Carlo simulations, while  $L_{\text{lat}}$  needs to be determined. Using the formalism of [17], we can express the transverse acceleration of charged leptons in the shower with energy  $\epsilon_e$  as  $d^2x_t/dt^2 = c^3 eB/[\epsilon_e \exp(-t/\tau)]$ , with  $x_t$ , the particle transverse position (orthogonal to the shower axis),  $\tau = l_{\text{rad}}/c$  the Bremsstrahlung energy loss timescale and  $l_{\text{rad}} = X_0/\rho_{\text{air}} \sim 3.67 \times 10^3 \text{ m} (\rho_{\text{air}}/1 \text{ g cm}^{-3})^{-1}$ , where  $X_0 = 36.7 \text{ g cm}^{-2}$  is the electronic radiation length. Integrating the transverse acceleration as a function of time we get  $x_t(t) = \tau^2 c^3 eB (e^{t/\tau} - 1 - t/\tau)/\epsilon_e$ . The shower lateral extent  $L_{\text{lat}}$  is then derived as  $L_{\text{lat}} = 2x_t(t = \tau)$ , where the factor 2 account for the deflection of both positrons and electrons. Hence, the coherence ratio which delimits the transition between coherent and incoherent emission yields

$$\frac{L_{\text{lat}}}{L_c} = \frac{\nu l_{\text{lat}}^2}{c D_{X_{\max}}} \sim 0.018 \left( \frac{\nu}{50 \text{ MHz}} \right) \left( \frac{B}{50 \mu\text{T}} \right)^2 \left( \frac{\epsilon_e}{88 \text{ MeV}} \right)^{-2} \left( \frac{\rho}{1 \text{ kg m}^{-3}} \right)^{-4} \left( \frac{D_{X_{\max}}[\rho]}{10 \text{ km}} \right)^{-1} \quad (2)$$

In the following, we will always consider charged leptons with an energy given by the critical energy  $\epsilon_e = 88 \text{ MeV}$ , since we want to consider the dynamics at  $X_{\max}$ . In the left-hand panel of Fig. 4, we represent with a grey solid line the coherence ratio as a function of air density at  $X_{\max}$  and shower zenith angle for GRAND magnetic field strength ( $B_{\text{GRAND}} = 56 \mu\text{T}$ ) at 50 MHz. We can see that for  $\rho_{\text{air}} \gtrsim 0.27 \text{ kg m}^{-3}$ , i.e. for  $\theta < 75^\circ$ , we have  $L_{\text{lat}}/L_c < 1$  and therefore expect coherent emission. However, for more inclined air-showers, i.e., for  $\rho_{\text{air}} \lesssim 0.27 \text{ kg m}^{-3}$  ( $\theta > 75^\circ$ ) we have a transition to a regime where  $L_{\text{lat}}/L_c > 1$  and incoherent emission is expected. In the right-hand panel of Fig. 4, the gray lines also indicate the transition between coherent (below the line) and incoherent emission (above the line), in the  $(\nu, \rho)$  phase space, for Auger (thin line) and GRAND (thick line) magnetic field configurations (respectively  $56 \mu\text{T}$  and  $25 \mu\text{T}$ ). Consistently with the Monte-Carlo predictions shown in Fig. 2, we find that the radio signal is more likely to loose coherence for strong magnetic field and at high frequencies.

#### 4.2 Conditions for synchrotron emission in the radio emission of air-showers

For low air-densities and high magnetic field values we also expect charged particles in the shower to undergo an enhanced magnetic deflection with associated synchrotron emission. We use the theoretical framework developed by C. James in [18] and assume that a non negligible synchrotron emission is expected if particles can radiate before losing their energy, i.e., for  $l_{\text{synch}}/l_{\text{rad}} < 1$ , with  $l_{\text{syn}} \sim 1157 \text{ m} (\epsilon_e/88 \text{ MeV})^{2/3} (B/50 \mu\text{T})^{-2/3} (\nu/80 \text{ MHz})^{-1/3}$ , the synchrotron cooling length derived in [18] and  $l_{\text{rad}} = \chi_0/\rho$ , the Bremsstrahlung energy loss length and. Hence

$$\frac{l_{\text{syn}}}{l_{\text{rad}}} \sim 3.7 \left( \frac{\epsilon_e}{88 \text{ MeV}} \right)^{2/3} \left( \frac{B}{50 \mu\text{T}} \right)^{-2/3} \left( \frac{\nu}{50 \text{ MHz}} \right)^{-1/3} \left( \frac{\rho}{1 \text{ kg m}^{-3}} \right). \quad (3)$$

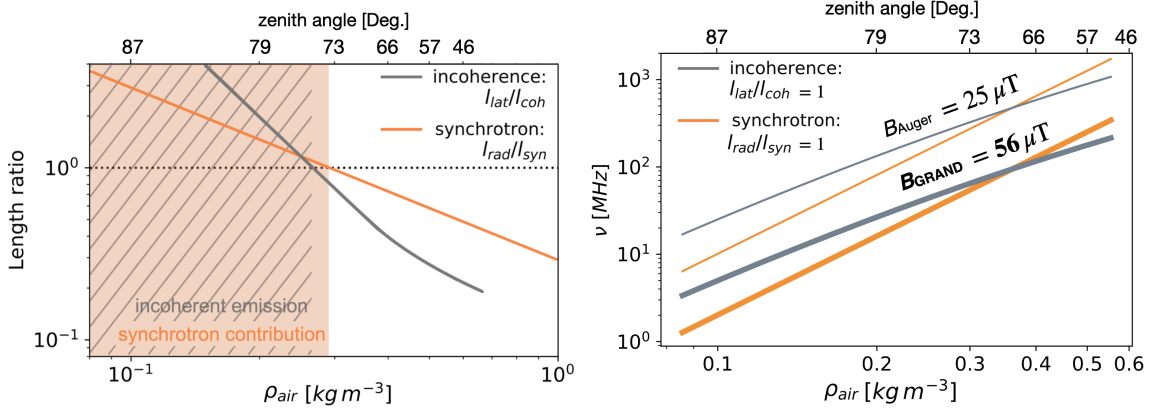


**Figure 4:** *Left:* Incoherence ratio  $L_{lat}/L_c$  (grey solid line) and synchrotron ratio  $l_{rad}/l_{syn}$  (orange solid line), versus air density at a frequency of 50 MHz, for GRAND site Dunhuang magnetic field configuration of  $B = 56 \mu\text{T}$ . The horizontal dotted line marks the limit where the ratios equal unity. *Right:* Incoherence and synchrotron transition limits (gray:  $l_{lat}/l_{coh} = 1$  and orange:  $l_{syn}/l_{rad} = 1$ ) versus frequency  $\nu$  and air density  $\rho_{air}$  for GRAND (thick lines) and Auger (thin lines) magnetic field configurations. In each case, a coherent [with significant synchrotron] is expected above the gray [orange] lines while no loss of coherence [no significant synchrotron contribution] are expected below the gray [orange] lines.

In the left-hand panel of Fig. 4, we represent with the orange solid line the synchrotron ratio as a function of air density and zenith angle, for GRAND magnetic field strength ( $B_{GRAND} = 56 \mu\text{T}$ ) at 50 MHz. We find that a significant synchrotron emission is expected, i.e.,  $l_{rad}/l_{syn} > 1$  for  $\rho_{air} \lesssim 0.29 \text{ kg m}^{-3}$  ( $\theta \gtrsim 73^\circ$ ). This prediction is consistent with the observations of the clover-leaf pattern for Monte-Carlo simulations of inclined air showers, as shown in Fig. 2. Finally, in the right-hand panel of Fig. 4, we show with an orange line the transition limit between a regime without any significant synchrotron emission (below the line) and with synchrotron emission (above the line), for GRAND (thick line) and Auger (thin line), magnetic field configurations. Similarly to what was observed with the coherence effects, we find that synchrotron emission is more easily generated at high frequencies and strong magnetic field amplitude.

## 5. Conclusion

Inclined cosmic-ray air-showers develop higher in the atmosphere than vertical ones which enhances the magnetic deflections of charged leptons in the cascade. In this study, we explored, with ZHAireS and CoREAS Monte-Carlo simulations, the radio emission of these inclined showers. We evidenced two major novel features: a suppression in the radiation energy and the emergence of a new polarization pattern at MHz frequencies for low air-densities and typical magnetic field strength of  $50 \mu\text{T}$ . We then developed a refined modeling of the air-shower radio emission to account for these new effects that we linked respectively to: a loss of coherence in the radio signal and an additional synchrotron contribution for inclined air-showers. Our results allowed us to evidence 3 distinct regimes as a function of air-density: (1) at high densities we retrieve a coherent transverse current emission as predicted by the former models, (2) at intermediate densities we find an additional coherent synchrotron contribution to the transverse current emission, (3) at the lowest

densities we find that an incoherent radio emission is expected. These regimes are highly dependent on the magnetic field amplitude and have strong implications: (1) they show that the current paradigm of radio signals made of a transverse current and a charge excess contribution only is no longer valid for inclined air-showers; (2) they show that the radio emission cut-off is site-dependent and could be used to either enhance the cosmic-ray detection or attenuate it, depending on the  $B_{\text{geo}}$  value. Particularly, as neutrino showers develop deeper in the atmosphere than cosmic-rays, their radio emission should not be subject to any cut-off. As a consequence, choosing a site with high magnetic field value could be interesting to perform cosmic-ray/neutrino discrimination.

## 6. Acknowledgements

The authors would like to thank Marion Guelfand, Olivier Martineau-Huynh, Pragati Mitra, Simon Prunet, Olaf Scholten and Washington R. Carvalho Jr for the fruitful discussions on the radio cut-off, Nikolaos Karastathis for his valuable input on the synchrotron emission with CORSIKA and the organizers of the ICRC conference for setting the event.

## References

- [1] D. Charrier *et al*, *Astroparticle Physics* **113**, 6–21 (2019).
- [2] W.D. Apel *et al*, *The European Physical Journal C* **81**, (2021).
- [3] A. Aab, *et al*, *Physical Review D*, **89**, pp.052002. (2014).
- [4] A. Corstanje *et al*, *Astroparticle Physics* **61**, 22–31 (2015).
- [5] T. Huege, *Physics Reports* **620**, 1–52 (2016).
- [6] F. Schroeder, *Progress in Particle and Nuclear Physics* **93**, 1–68 (2017).
- [7] J. Álvarez-Muñiz *et al*, *Science China Physics, Mechanics & Astronomy* **63**, (2019).
- [8] B. Pont *et al*, *PoS ICRC2019*, 395 (2019).
- [9] S. Chiche *et al*, *Astroparticle Physics* **139**, 102696 (2022)
- [10] F. Schlüter and T. Huege, *Journal of Cosmology and Astroparticle Physics* **2023**, 008 (2023).
- [11] F. Schlüter *et al*, *The European Physical Journal C* **80**, 643 (2022).
- [12] T. Huege *et al*, *International Cosmic Ray Conference* **36**, 294 (2019).
- [13] Jaime Alvarez-Muñiz *et al*, *Astroparticle Physics* **35**, 6, 325–341, (2012)
- [14] C. Glaser *et al*, *Journal of Cosmology and Astroparticle Physics* **2016**, 09, 024–024, (2016)
- [15] S. Chiche *et al*, *37th International Cosmic Ray Conference*, 194 (2022).
- [16] T. Huege *et al*, *5th International Workshop on Acoustic and Radio EEV Neutrino Detection Activities* **1535**, 128-132 (2013).
- [17] O. Scholten *et al*, *Astroparticle Physics* **29**, 2, 94–103, (2008)
- [18] C. James, *Physical Review D* **105**, 2 (2022)
- [19] T. Huege and H. Falcke, *Astronomy & Astrophysics* **430**, 3, 779–798, (2004)
- [20] J. Hörandel, *Proceedings of 37th International Cosmic Ray Conference — PoS(ICRC2021)*, (2021).
- [21] S. Chiche *et al*, *Proceedings of 9th ARENA conference — PoS(ARENA2022)* **035**, (2022).
- [22] T. Huege, *Proceedings of 9th ARENA conference — PoS(ARENA2022)* **053**, (2022).